EXPERIMENTAL STUDIES OF HIGH STRAIN RATE TENSILE BEHAVIOUR OF MATERIALS

A Thesis Submitted
In Partial Fulfilment of the Requirements
for the Degree of
MASTER OF TECHNOLOGY

By

Lt. N. K. RAO

to the
DEPARTMENT OF MECHANICAL ENGINEERING
INDIAN INSTITUTE OF TECHNOLOGY KANPUR
JULY, 1983

ME-1983-M-RAO-EXP

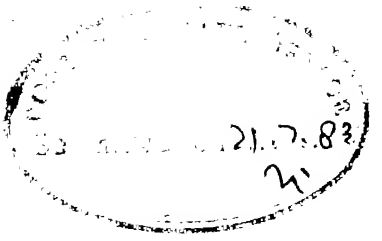

CERTIFICATE

This is to certify that the thesis entitled " Experimental Studies of High Strain Rate Tensile Behaviour of Materials" submitted in partial fulfilment of the requirements for the Degree of Master of Technology by Lt. N.K. Rao, is a record of work carried out under my supervision and has not been submitted elsewhere for a degree.

Prashant Kumar

(PRASHANT KUMAR)
ASSISTANT PROFESSOR
DEPARTMENT OF MECHANICAL ENGG.
INDIAN INSTITUTE OF TECHNOLOGY
KANPUR-208016, INDIA

ACKNOWLEDGEMENT

I express my deep sense of gratitude and appreciation to Dr. Prashant Kumar, for his invaluable guidance and constant encouragement throughout the present work.

I am also grateful to Dr. B.D. Agarwal for his timely suggestions throughout the duration of this present work. A special word of appreciation is due to Mr. R.K. Nakrani, whose help and guidance proved immense throughout the experimental phase of the present work. Credit is due to Mr. L.J. Rao and Mr. D.K. Sarkar for their active participation.

It is with pleasure that I recall my association with Capt. K.S. Choudary, Mr. K.V. Subba Rao and Mr. Sarat Babu for their constructive suggestions and help.

A word of thanks and appreciation to Mr. S.L. Srivastava, Mr. Dwivedi and Mr. R.S. Shukla for their cooperation and help, during the fabrication stage of the present work.

Last but not the least, a word of praise for Mr. D.P. Saini, for his excellent typing.

KRISHNA

LIST OF CONTENTS

			Page
CERTIFICATE			i
ACKNOWLEDGEMENT			ii
LIST OF FIGURES			iv
ABSTRACT			v
CHAPTER-1	:	INTRODUCTION	1
CHAPTER-2	:	THEORETICAL FORMULATION	6
CHAPTER-3	:	EXPERIMENTAL TECHNIQUE	17
3.1	:	Pressure Bars and Striker	17
3.2	:	Specimen and its Loading	21
3.3	:	Strain Gauges	26
3.4	:	Oscilloscope	30
CHAPTER-4	:	EXPERIMENTAL RESULTS	33
4.1	:	Aluminium Specimen	34
4.2	:	Unidirectional Glass Fibre Reinforced Composite Specimen	44
4.3	:	Summary	45
CHAPTER-5	:	CONCLUDING REMARKS	48
REFERENCES			51

LIST OF FIGURES

Figure No.		Page
2.1	Schematic Diagram of Kolsky Bar Set-up	7
2.2	Time-Distance Diagram	9
3.1	Overall View of Kolsky Pressure Bar Set-up	18
3.2	Details of the Pressure Bars	20
3.3	Details of a Specimen	22
3.4	Photograph Showing a Specimen, a Collar and the Ends of Pressure Bars	23
3.5	Hard Copy Recorded on Hewlett-Packard Recorder	25
3.6	Bridge Circuit to Record Strain Pulse in the Pressure Bars	28
3.7	A Typical Oscilloscope Record of the Aluminium Specimen Tested by Kolsky Bar Technique (Hard Copy of the Oscilloscope Record is Shown in Fig. 3.5)	32
4.1	Stress-Strain Curves for Aluminium	36
4.2	Specimen No. 6 (Upper) Deformed at a High Strain Rate of 810s^{-1} and an Untested Specimen (Lower)	40
4.3	Yield Stress Vs Average Strain Rate for Aluminium	41
4.4	Comparison of Results With Results of Theodore Nicholas	43
4.5	Transverse Tension Test on a Uniaxial GFRP Specimen	46

ABSTRACT

A technique to determine stress-strain behaviour of a material, at high strain rates under tension, has been developed. A short specimen along with a collar, was pulled between two elastic bars and was subjected to a tensile loading pulse of approximately 116μs duration. Incident, reflected and transmitted pulses were recorded through strain gauges on a digital oscilloscope, fixed on pressure bars for subsequent analysis.

Stress-strain curves of commercially available aluminium metal between the strain rates of $410s^{-1}$ and $810s^{-1}$, were obtained using the above mentioned technique. The behaviour of stress-strain curves at different strain rates, confirmed the strain rate sensitivity of aluminium metal at room temperature. It was observed that strain hardening is small, specially at a high strain of the order $560s^{-1}$. The dynamic yield stress is observed to depend significantly on strain rates between $410s^{-1}$ and $810s^{-1}$.

CHAPTER - 1

INTRODUCTION

Numerous applications of structural materials involve dynamic or impact type of loading. In order to design or analyse dynamically loaded structures more accurately, it is necessary to know the mechanical properties of materials at various strain rates. The mechanical behaviour of most materials is known to be dependent upon the rate of deformation in addition to other factors such as temperature, strain history and structure. The study of dynamic behaviour of materials is important from several points of view, such as fabrication, cutting, failure criterion, strength and mode of failures etc. Furthermore during collisions, material is stronger than what is predicted by conventional tests for example an Aeroplane body can withstand high contact stresses when a large bird heats its body.

The experimental determination of a material behaviour at high strain rates is difficult problem. The test system should be capable of producing the required dynamic loads in a known way and of measuring

the response of material without itself affecting material behaviour. The conventional type of material testing machines such as M.T.S. and Instron can produce a maximum strain rate only of the order of 10^{-1} sec^{-1}. Therefore, unconventional methods have to be devised for study at high strain rates of the order of 10^{3} sec^{-1}.

Kolsky[1] developed a technique in 1949 to determine material properties at high strain rate of loading. In this technique, a short and cylindrical specimen is sandwiched between two long, hard and elastic bars of circular cross-section. The specimen is loaded in compression by passing a stress pulse generated by a detonator, which imparts velocity to the striker Bar. This technique is also being referred as Kolsky pressure Bar technique.

Davies and Hunter[2] (1963) has made a complete experimental and theoretical study of Kolsky pressure Bar technique, which rather clearly defines its limits of application. They adopted small specimen and the apparatus used, employs explosively loaded anvil bar in contact with a disc specimen, whose second face is in contact with a steel bar. Specimen is subjected to a loading cycle of 30μ sec. duration with a rise time of 10-15μ sec. They studied the behaviour of some metals like annealed copper, aluminium, magnesium and polymers.

Lindholm[5] (1964) has conducted experiments on Kolsky pressure bar technique to determine the strain rate sensitivity of lead, aluminium, and copper. The loading pulse is initiated by axial impact from a striker bar which is accelerated to impart velocity by a sling shot type mechanism in which driving force is supplied by torsion spring. Loading pulse of duration of 100μ sec. is generated and material behaviour in compression was studied.

Hauser[6] (1966) described a tension version of Kolsky pressure bar technique, which involved generating a compression pulse in a tube surrounding a solid inner rod. The tube and rod are connected by a mechanical joint. When the compression pulse in the outer tube reaches the joint which is a free end, it reflects back through the solid inner rod as a tensile pulse. A threaded tensile specimen is attached to the inner rod to provide the mechanical connection necessary to transfer the tensile pulse through the specimen, into a second rod. Strain rates of over 1000 s^{-1} were achieved in such an apparatus where loading eccentricity is minimized. Although, this is a direct method for generating high strain rate data in tension, the technique suffers from the inability to generate tensile waves having very short rise times, because of wave dispersion at mechanical joint.

Lindholm and Yeakley[7] (1968) extended Kolsky technique and obtained complete stress-strain curves at strain rates of order of 1000sec^{-1}, in tension and compression. The tensile specimen is hat shaped, placed between a solid cylindrical incident bar and tubular transmitter bar. Though the experiment is easy to perform, specimen design is complex which required considerable machining. Stress strain curves for 1100-0 aluminium have been presented. For very low strain rates, the stress levels in tension and compression agree, although the increase in flow stress with increasing strain rate differs in detail.

Jashman[9] (1971) has applied one dimensional elastic wave propagation analysis to assess the validity of Kolsky formulae for measuring dynamic behaviour of material . He showed that one dimensional effects dominate, by careful selection of design parameters such as specimen length and pulse shape, one may use the Kolsky formulae with sufficient accuracy.

Amijma Sadao and Toru Fujii[15] (1976) have conducted experiments on glass fiber composite materials. They prepared specimen by laying fiber cloth parallel to each other in epoxy matrix. Strength of such composites increases with increase in strain rate and with increase in volume fraction.

Theodre Nicholas[11] (1981) developed a tensile version of Kolsky pressure bar technique for high strain rates. This is a simple laboratory apparatus for high strain rate tensile testing. He conducted tests in tension upto strain rates of 10^3 sec^{-1}. In this apparatus, pressure bars are snug against a collar, and a threaded specimen is screwed between them. Generated compressive pulse passes through collar to the second bar and returns as tensile pulse from its free end. Specimen is loaded by tensile pulse. He conducted tests on aluminium and lead.

The main objective of the present work is, to develop a Kolsky pressure bar setup to carry out high strain rate tensile testing, which involves the design and fabrication of pressure bars and specimen. The above technique was perfected on aluminium specimen. Preliminary investigations were carried out on fiber composite material .

The thesis is organized as follows:

(i) Theoretical formulation is described in Chapter-2.

(ii) Experimental technique is described in Chapter-3.

(iii) Experimental results are discussed in Chapter-4.

(iv) Concluding remarks are given in Chapter-5.

CHAPTER - 2

THEORETICAL FORMULATION

Kolsky pressure bar technique is based on one dimensional wave propagation in the circular pressure bars. Under the application of shock load, the bars remain elastic and work like a wave guide. Stress waves propagate in the bar with the velocity of $\sqrt{E/\rho}$ where E is the Youngs Modulus and ρ is the density of bar material. When a short specimen is loaded between two elastic bars, its ends move with different velocities and it leads to deformation of specimen. As the shock front enters the short specimen, it reverberates and makes the stress more or less uniform in a short time. The entire information about stress, strain rate and strain in the specimen can be obtained by measurement of stress waves alone, in the elastic bars. Kolsky bar technique is shown schematically in Fig. 2.1. The apparatus essentially consists of two long and circular bars termed as bar No. 1 and bar No. 2. Striker bar is accelerated against bar No. 1 by an air gun. Specimen is subjected to tensile loading due to reflected pulse from free end of bar No. 2.

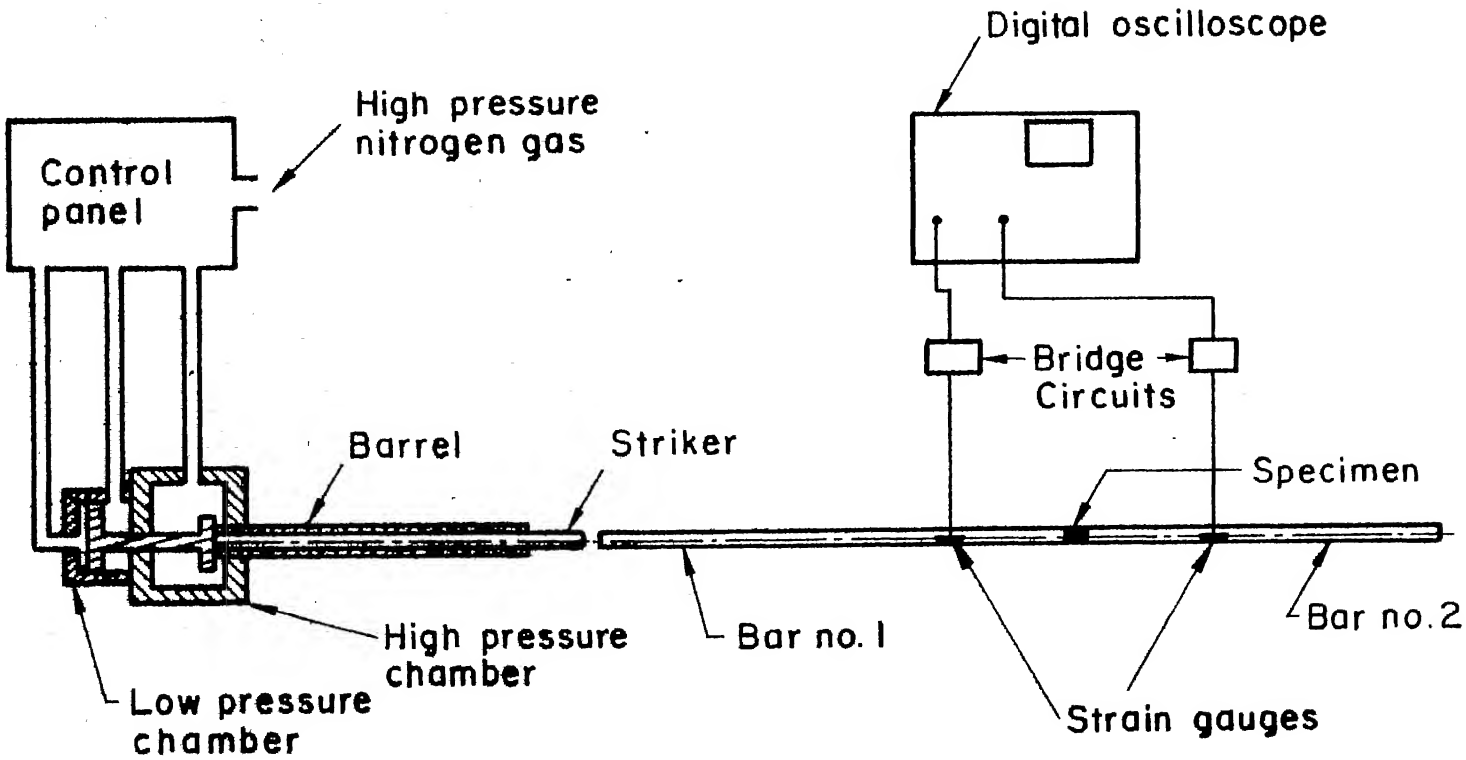

Fig. 2.1 Schematic diagram of Kolsky bar set up

The two pressure bars act as a means of loading the specimen and also as transducers to measure the stress levels. The strain gauges mounted on the bars give the stress history.

For a stress wave propagation in one direction a time distance diagram is very useful for design purposes such as, finding lengths of bars and location of strain gauges. Stress wave propagation in the bars are shown conveniently through a time distance diagram in Fig.2.2. Distance 'x' is chosen along horizontal axis, while time 't' is chosen along the vertical axis. For better visualization the striker, bar No. 1 and bar No. 2 along with a specimen have been drawn above t-x diagram. Time 't' is measured from the instant the front end of striker touches bar No. 1.

At the instant of impact, compressive waves start propagating in the bar No. 1 as well as in the striker, with sound velocity. The state of stress 'σ' and particle velocity v, are governed by conservation of momentum, equations of strain-displacement, and constitutive relations. Simple relations are obtained along the characteristic directions having slopes +c and -c. The relations along the characteristics are:

$$d\sigma - \rho c\, dv = 0 \quad \text{along } +c \text{ characteristic}$$

$$d\sigma + \rho c\, dv = 0 \quad \text{along } -c \text{ characteristic}$$

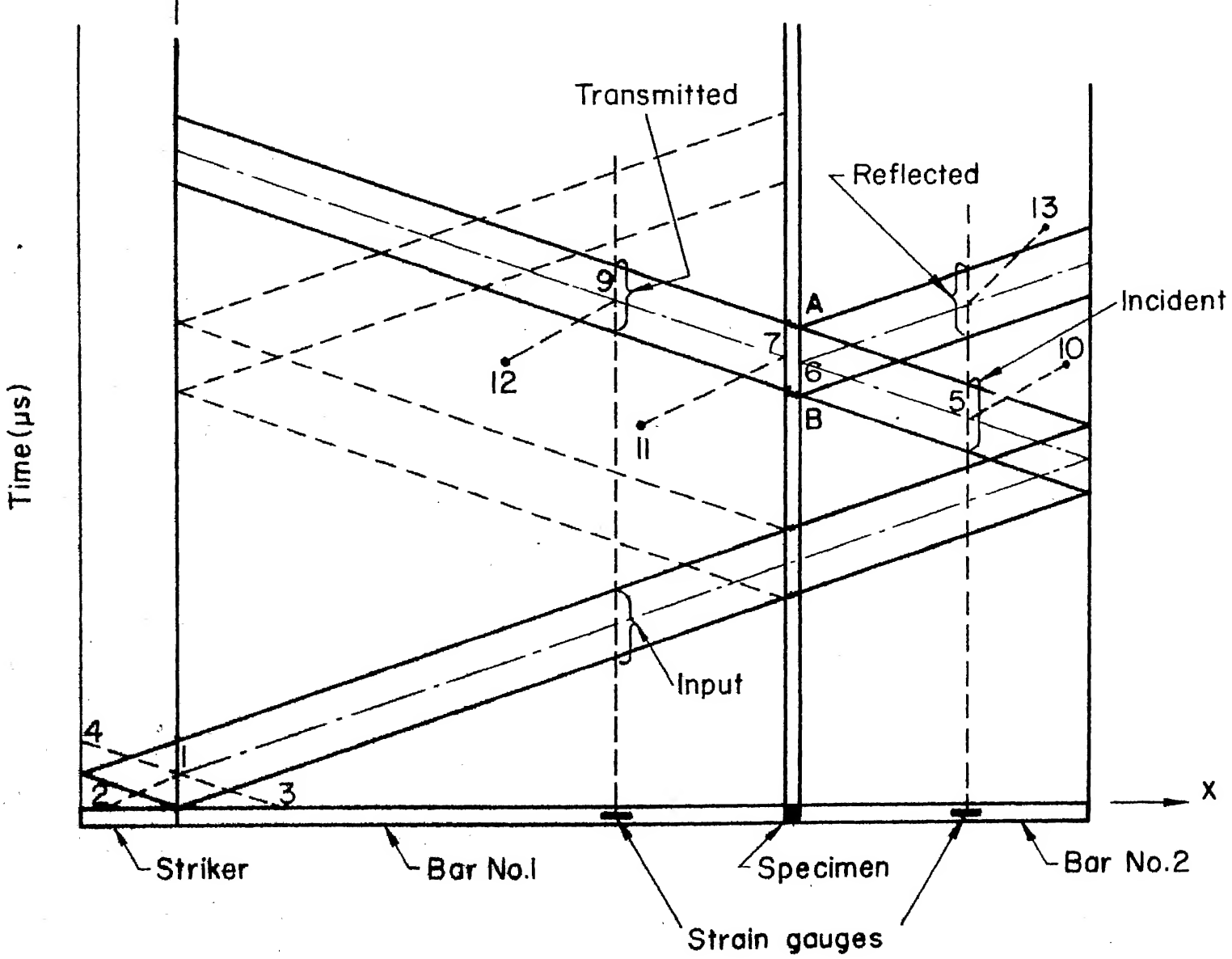

Fig. 2.2 Time - distance diagram

The product ρc plays very important role because it relates stress with particle velocity and is generally known as acoustic impedance. State of stress at the impact interface between the striker and bar No. 1 is evaluated by writing relations between points 1, 2 and 3. Noting that for the striker just before the impact, stress $\sigma = 0$ and particle velocity v is equal to 'V' , one obtains

$$\sigma_1 - \rho c v_1 = \sigma_2 - \rho c v_2$$
$$= 0 - \rho c V \qquad (2.1)$$

Relation along the characteristic 1-3 is

$$\sigma_1 + \rho c v_1 = \sigma_3 + \rho c v_3$$
$$= 0 \qquad (2.2)$$

because stress and particle velocity of the bar No. 1 at $t = 0$ are zero. Solving equations (2.1) and (2.2) one obtains

$$\sigma_1 = - \frac{\rho c V}{2} \qquad (2.3)$$

and $v_1 = V/2$

The negative sign signifies that the stress is compressive. This state of stress at the impact interface between the striker and the input bar is unchanged until a wave front arrives after being reflected from the end of one of two bars. Since the striker is shorter in

length, the compressive wave front encounters its free surface ($\sigma = 0$) and is reflected back into the bar to reach the impact face shown by characteristic B-C in Fig.2.1. Particle velocity at the point 11 is found by equations

$$\sigma_4 + \rho c v_4 = \sigma_1 + \rho c v_1 \qquad (2.4)$$

or $$0 + \rho c v_4 = - \frac{\rho c V}{2} + \frac{\rho c V}{2} \qquad (2.5)$$

or $$v_4 = 0$$

which means, the striker attains zero velocity and zero stress once the reflected pulse wave front sweeps the striker. Consequently, after twice the propagation time in striker the interface at $x = 0$, no longer has any compressive stress. The compression which acts on the impact interface for the time interval $2l_s/c$ (l_s = length of striker) takes shape of a compressive pulse in the bar No. 1. The boundary condition at the interface should generate a square pulse in the bar No. 1, with very small rise time, but the front of the stress pulse disperses due to geometric factors as it travels in the bar.

The pulse propagates with the speed of sound 'C' in the bar No. 1 and transmitted to bar No. 2 through an elastic collar around the specimen. The collar can transmit only compressive waves, as its faces are not

glued to the bars No. 1 and 2. Also, a most of the compressive pulse propagates through the collar and the rest through the specimen as cross-sectional area of collar is chosen to be considerably larger than that of the specimen. Thus, the specimen is not subjected to high stress. The pulse transmitted to bar No. 2 through collar, reflects back from the bar No. 2 as a tensile wave and it propagates with speed of sound till it hits the specimen. The tensile pulse has no other alternative but to pass through the specimen, as the collar can not take tensile load. Due to difference in acoustic impedance, part of the tensile pulse is reflected back into bar No. 2 and rest is transmitted to the bar No. 1. Within the specimen, several reverberations of the stress waves (elastic and plastic) between two elastic bars, makes the state of stress nearly uniform.

Stresses of incident and reflected pulses are recorded by strain gauges fixed on bar No. 2. Stress level of transmitted pulse is recorded by strain gauges fixed on bar No. 1. Stresses and particle velocities at points 6 and 7 of Fig. 2.2 are evaluated from the strain gauges fixed on bar No. 1 and bar No. 2. Relations along characteristic 5-6

$$\sigma_5 + \rho c v_5 = \sigma_6 + \rho c v_6 \qquad (2.6)$$

and along 5-10 is

$$\sigma_5 - \rho c v_5 = \sigma_{10} - \rho c v_{10} = 0 \qquad (2.7)$$

Eliminating v_5 from eqns. (2.6) and (2.7) we obtain,

$$\sigma_6 + \rho c v_6 = 2\sigma_5 \qquad (2.8)$$

Similarly, relations along characteristic 6-8 and 8-13 are

$$\sigma_6 - \rho c v_6 = \sigma_8 - \rho c v_8 \qquad (2.9)$$

$$\sigma_8 + \rho c v_8 = \sigma_{13} + \rho c v_{13} = 0 \qquad (2.10)$$

and they are simplified to

$$\sigma_6 - \rho c v_6 = 2\sigma_8 \qquad (2.11)$$

Equations (2.8) and (2.11) yield

$$\sigma_6 = \sigma_5 + \sigma_8 \qquad (2.12)$$

and

$$v_6 = \frac{\sigma_5 - \sigma_8}{\rho c} \qquad (2.13)$$

Similarly σ_7 , v_7 can be evaluated in terms of measured stress σ_9. Relations along characteristics 7-9, 7-11, 9-12 are

$$\sigma_7 + \rho c v_7 = \sigma_9 + \rho c v_9 \qquad (2.14)$$

$$\sigma_7 - \rho c v_7 = \sigma_{11} - \rho c v_{11} = 0 \qquad (2.15)$$

$$\sigma_9 - \rho c v_9 = \sigma_{12} - \rho c v_{12} \qquad (2.16)$$

Solving above three equations, it can be shown that

$$\sigma_7 = \sigma_9 \tag{2.17}$$

$$v_7 = \sigma_9/\rho c \tag{2.18}$$

Since Equations (2.13) and (2.18) express particle velocities on end faces of specimen i.e. point 6 and point 7 of Fig. 2.2, the strain rate is expressed by following relation

$$\dot{\varepsilon} = \frac{v_6 - v_7}{h} \tag{2.19}$$

where h is thickness of specimen.

From Eqns. (2.13) and (2.18) it can be shown that

$$\dot{\varepsilon} = \frac{\sigma_5 - \sigma_8 - \sigma_9}{\rho ch} \tag{2.20}$$

and average stress in specimen is

$$\bar{\sigma} = \frac{\sigma_6 + \sigma_7}{2}$$

or,
$$\bar{\sigma} = \frac{\sigma_5 + \sigma_{12} + \sigma_7}{2} \tag{2.21}$$

Incident, reflected and transmitted pulses are indicated by symbols I, R, and T respectively. Equations (2.20) and (2.21) can be rewritten as

$$\dot{\varepsilon} = \frac{\sigma_I - \sigma_R - \sigma_T}{\rho ch} \tag{2.22}$$

$$\bar{\sigma} = \frac{\sigma_I + \sigma_T + \sigma_R}{2} \tag{2.23}$$

Strain is determined by integrating the equation (2.22) expressed as follows

$$\varepsilon = \int_0^t \frac{(\sigma_I - \sigma_R - \sigma_T)}{\rho c h} dt \qquad (2.24)$$

For materials, whose sound velocity C and acoustic impedance ρc are small and deform plastically when shock load is applied, equations (2.20) and (2.21) can be simplified by assuming.

$$\sigma_6 = \sigma_7 \qquad (2.25)$$

Equations (2.12) and (2.14) give

$$\sigma_8 = \sigma_9 = \sigma_5 \qquad (2.26)$$

Substituting (2.25) and (2.26) in equations (2.20) and (2.21) we can obtain

$$\dot{\varepsilon} = \frac{2(\sigma_5 - \sigma_9)}{\rho c h} = \frac{2(\sigma_I - \sigma_T)}{\rho c h} \qquad (2.27)$$

average stress equation becomes

$$\bar{\sigma} = \sigma_9 = \sigma_T \qquad (2.28)$$

and strain gauge fixed on bar No. 1 directly records stress in the specimen.

This technique has a limitation,as in the first few reverberations in the specimen,stress is nonuniform and low. Therefore, stress-strain relations of a specimen are not determined for low strains. This is not a

serious drawback,as most of the materials remain elastic at low strains and elastic behaviour does not depend appreciably on strain rates. However, in the range of plastic deformation, the stress within the specimen is nearly uniform and the experimental results are valid.

CHAPTER - 3

EXPERIMENTAL TECHNIQUE

Kolsky pressure bar apparatus is shown schematically in Fig. 2.1 and overall view of setup is shown in Fig. 3.1. This apparatus, principally consist of a striker, two long elastic mild steel bars, strain gauges associated Bridge circuits and oscilloscope. The loading pulse in the experiments is initiated by axial impact from a striker bar, which is accelerated to impart velocity by an Air gun. The Air gun employed has 20 mm bore and powered by compressed Nitrogen. The gun is fired with the help of a control panel, such that the Nitrogen gas is released quickly through the barrel[16].

3.1 PRESSURE BARS AND STRIKER

Striker, bar No. 1 and bar No. 2 are made of 18 mm diameter cold rolled mild steel which remain elastic during impact. The bars are aligned along the axis of the gun barrel. Striker has diameter of 19.7 mm and bar length of 292 mm. The striker generates a compressive pulse whose amplitude depends on the striker velocity and whose length is twice the longitudinal elastic wave

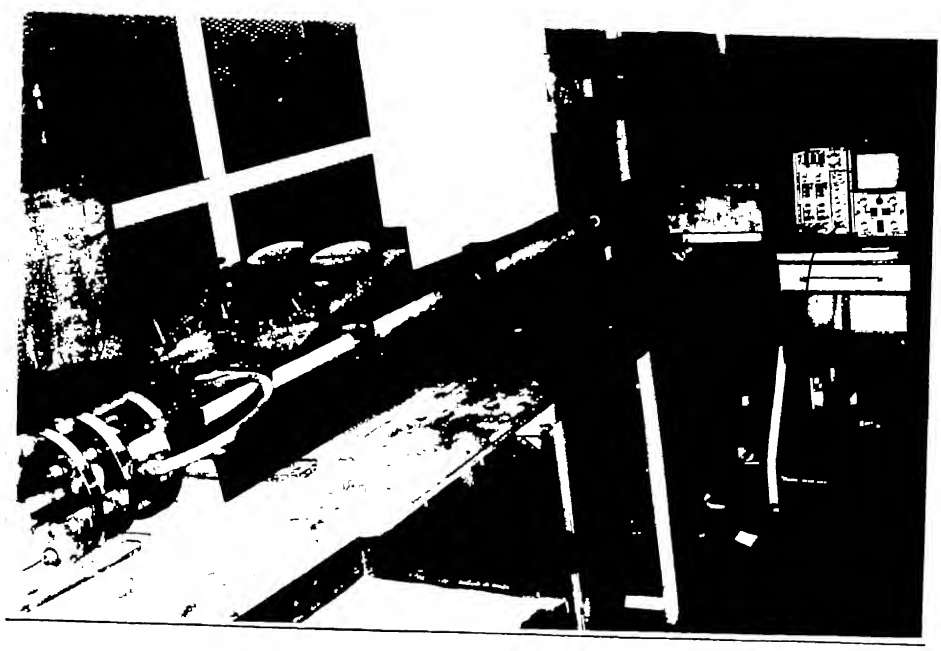

FIG. 3.1 : OVERALL VIEW OF KOLSKY PRESSURE BAR SETUP.

transit time. In order to minimize the effect of any misalignment, the front face of striker is machined into a spherical shape with a radius fifteen times that of a bar. This ensures that a misaligned striker will always make a point contact on the flat face of bar No. 1. Although the rounded front face of striker bar gives slowly rising ramp type of shock front, it does not cause any problem, as shock front in a bar has its own rise time. For the 18 mm Kolsky bars, the rise time is 16μs, which is large enough to absorb irregularities due to the rounded end of striker bar. Duration of compressive pulse is 116μs.

Details of the pressure bars i.e. bar No. 1 and bar No. 2 are shown in Fig. 3.2. Each pressure bar is supported by two teflon bearings as they do not restrict the passage of pulse due to their low acoustic impedance. The cross section of each bar near specimen end has been increased to 28 mm diameter for a length of 60 mm. This is done to hold thick specimen upto 18 mm diameter along with the elastic collar. It should be noted that pressure bars can not be chosen of uniform diameter of 28 mm, because the rise time of the pulse will be very large and the strain in the pressure bars will become low and will start giving noise problems in recording signals.

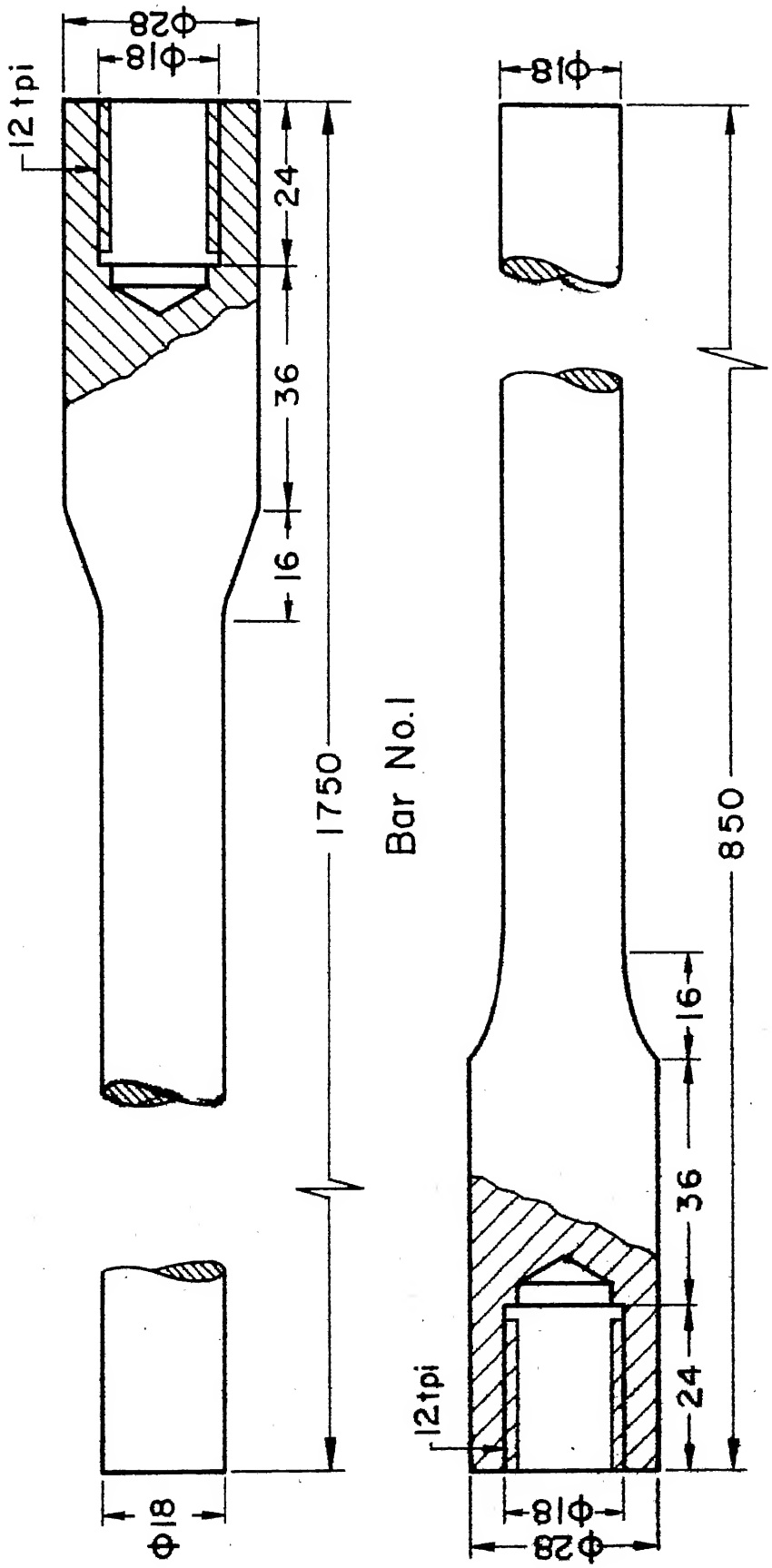

Fig. 3.2 Details of the pressure bars

Ends of the bars are drilled and internal threads have been made to hold specimen. The faces of pressure bars in contact with specimen are ground flat and parallel. The bar No. 1 has been chosen very long to avoid interference between stress pulses i.e., incident, reflected and transmitted.

3.2 SPECIMEN AND ITS LOADING

Most of the experiments have been carried out on commercially available aluminium of HINDALCO, Remikut, U.P. Dimensions of a specimen are as shown in Fig. 3.3. A collar made of same material (cold rolled mild steel) as pressure bars and is slipped over specimen. The collar has same outer diameter of 28 mm, same as outer diameter of pressure bars and has an internal diameter of 18.5 mm, just sufficient to clear the specimen. The ratio of area of collar and net cross sectional area of specimen is 3:1. Specimen is screwed in until pressure bars are snug against collar as shown in Fig. 3.4.

The compression pulse generated by striker in bar No. 1 travels through composite cross section of collar and specimen, in an essentially undispersed manner. Most of the energy of the compression pulse passes through the steel collar and the specimen remains elastic.

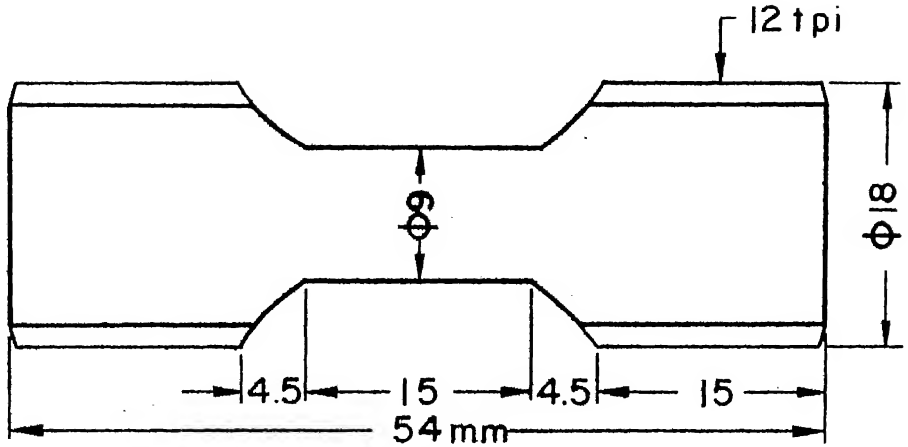

Fig. 3.3. Details of a specimen

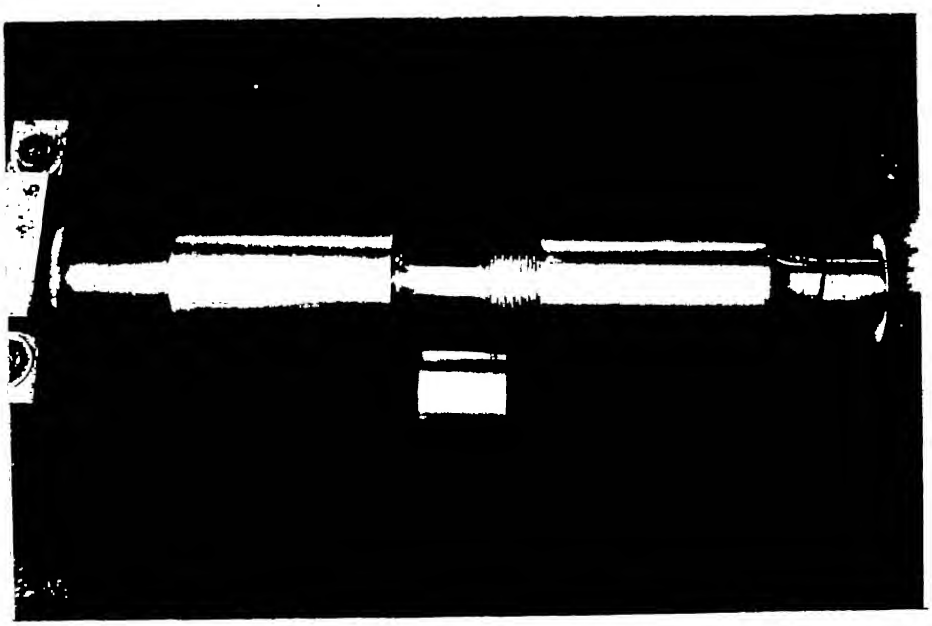

FIG. 3.4 : PHOTOGRAPH SHOWING A SPECIMEN, A COLLAR AND THE ENDS OF PRESSURE BARS.

This is because, the acoustic impedance of the steel collar is three times more than that of an aluminium specimen and the cross sectional area of the collar is three times bigger than that of the specimen. In effect, the entire compression pulse passes through supporting collar as if specimen were not present. The compression pulse continues to propagate until it reaches the free end of bar No. 2. Due to stress free boundary condition of the free end, it reflects and propagates back as tensile pulse shown as incident pulse in Fig. 3.5. The duration and shape of incident tensile pulse remains same as input pulse. This incident pulse upon reaching specimen is partially transmitted and partially reflected back into bar No. 2.

Note that, the collar which carried the entire compressive pulse is unable to support any tensile pulse, because it is not fastened in any manner to the bars. The snug fit of the threaded tensile specimen against the bars is absolutely essential in achieving a smooth and rapid loading of specimen as the tensile pulse arrives. Failure to remove all play out of threaded joint results in uneven loading of specimen and spurious wave dispersion.

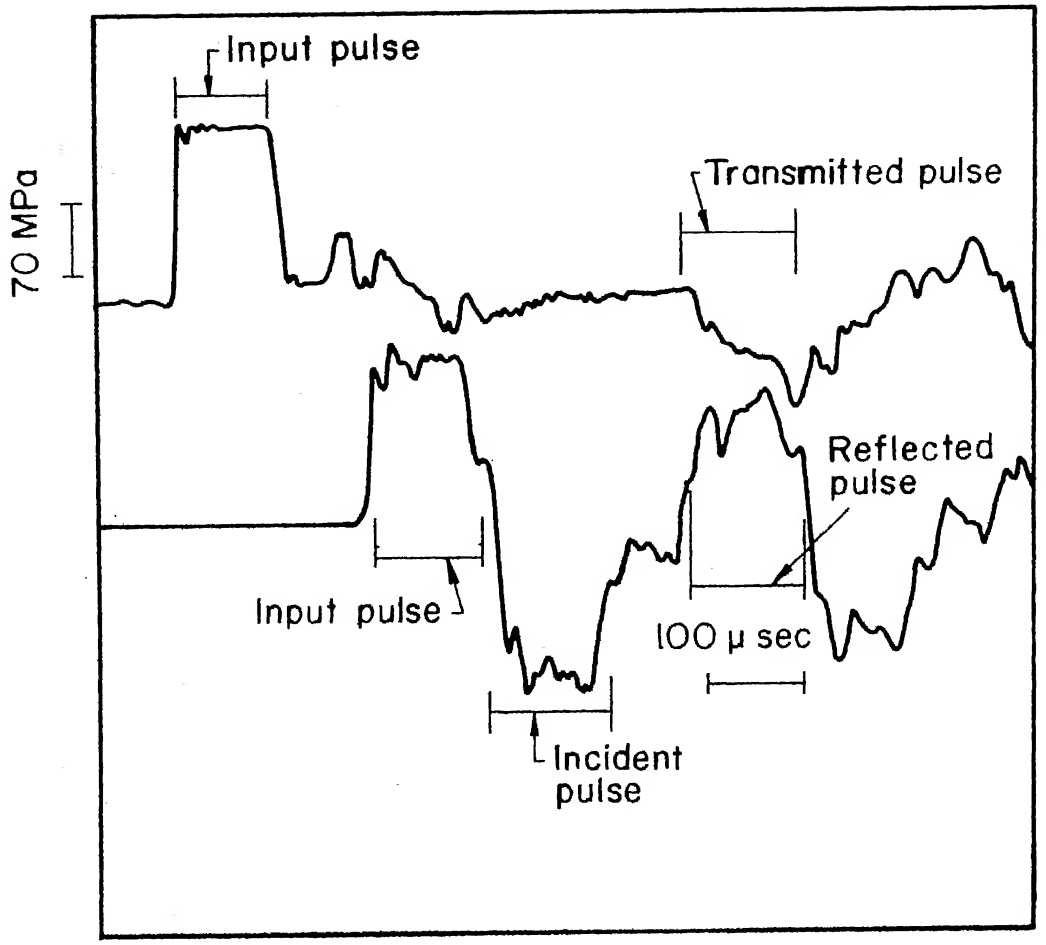

Fig.3.5 Hard copy recorded on Hewlett-Packard x-y recorder

3.3 STRAIN GAUGES

The pulses are recorded by means of resistance strain gauges mounted on the radial surfaces of pressure bars. On each pressure bar, two strain gauges are mounted diametrically opposite to each other and by using proper bridge circuit, flexural effects if any, are cancelled.

The location of strain gauges is important so that records can be obtained of each pulse without interference from reflected pulses. For this reason, the gauges are positioned so that distance between each gauge and the ends of respective pressure bars is greater than the length of striker bar. On the bar No. 1, strain gauges are fixed at 500 mm from the interface of specimen to record generated compression pulse and transmitted tensile pulse. On the bar No. 2, strain gauges are fixed at 500 mm from the interface of specimen to record incident tensile pulse and reflected pulse. For a striker of 292 mm length, the incident pulse will cross the gauges fixed on bar No. 2 by the time reflected pulse from the specimen reaches the strain gauges and thus pulses are separately recorded. By virtue of placement of strain gauges equidistant from the specimen on both pressure bars, the reflected pulse and transmitted pulse become time coincident.

Stress waves are mainly longitudinal type in this kind of experiment. But,due to eccentric impact between the striker and the bar No. 1, flexural waves may generate. Although the net effect of flexural waves on average stress and strain is negligible, the effect has to be cancelled while measuring stress through strain gauges. The wheat stone bridge is ideal for measuring strains.

Fig. 3.6 shows the strain gauge Bridge circuit. Two strain gauges are glued diametrically opposite on each pressure bar and they form the opposite arm of R_2 , R_4 of the wheat stone bridge. Each gauge is of 120Ω resistance. Resistance R_3 of bridge circuit corresponds to a dummy strain gauge mounted on a small metal rod of same diameter as that of pressure bars. It is identical to active gauges in size and resistance. Resistance R_1 corresponds to a constant resistor of 100Ω connected in series with 50Ω potentiometer. Another 2KΩ precession potentiometer is connected in parallel to the 50Ω potentiometer. The 50Ω and 2KΩ potentiometers provide coarse and fine balances respectively.

Another resistor of high resistance R_c along with shorting push button is connected in parallel with the strain gauge R_2. The calibaration resistor R_c is

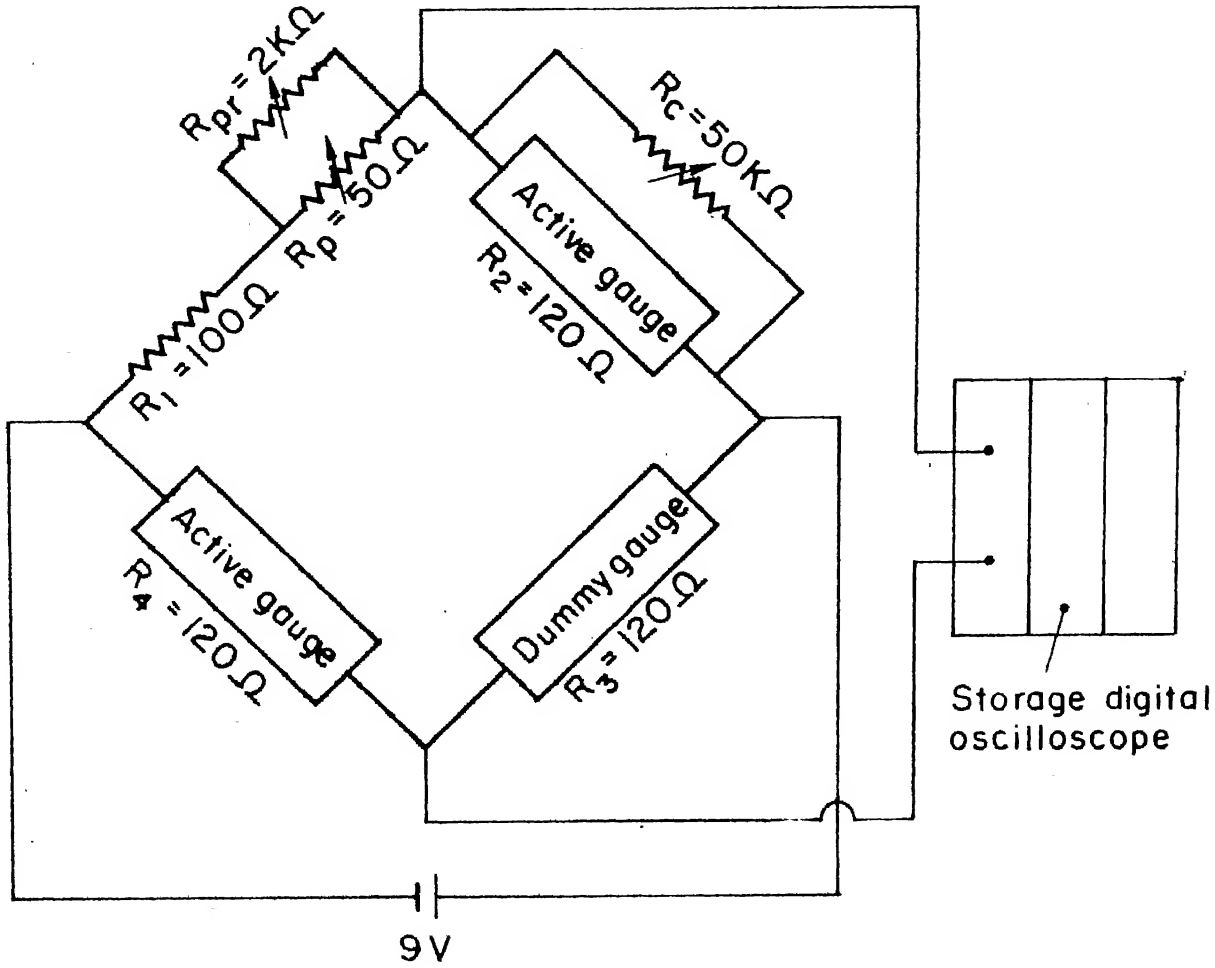

Fig. 3.6 Bridge circuit to record strain pulse in the pressure bars.

of variable type. When the push button is shorted, the resistance across the gauge R_2 changes, which in turn gives an output on the oscilloscope. Thus it gives a direct calibaration relation between resistance change of the gauge and voltage deflection V_c on oscilloscope.

Before every measurement a null point is obtained by controlling the potentiometers.

Then $\Delta E = 0$

or $E_1 = E_2$

or, $$\frac{R_2 V}{R_1+R_2} = \frac{R_3 V}{R_3+R_4}$$

or, $R_1 R_3 = R_2 R_4 = R^2$ since $R_2 = R_4 = R$.

When the caliberation resistor R_c is connected in parallel to strain gauge R_2 by push button, the equivalent resistance R_{2e} becomes

$$R_{2e} = \frac{R_2 R_c}{R_2+R_c}$$

and the overall resistance change ΔR_2 is

$$\frac{\Delta R_2}{R_2} = \frac{R_{2e} - R_2}{R_2}$$

which gives,

$$\frac{\Delta R_2}{R_2} = \frac{-R_2}{R_2 + R_c}$$

The gauge factor S_g of the strain gauges is defined by

$$S_g = \frac{\Delta R_2 / R_2}{\varepsilon}$$

where S_g is the strain in the gauge. Therefore, the strain ε_c induced due to change in R_2 is

$$\varepsilon_c = - \frac{R_2}{S_g (R_2 + R_c)}$$

corresponding to this strain, caliberation voltage V_c is directly read from the oscilloscope screen. Since the stress pulses are monitored through two gauges, the voltage output is double for the same strain.

3.4 OSCILLOSCOPE

A dual beam digital oscilloscope made by Nicolet Corporation (Model 2090, Explorer-II) is used to record the strain gauge signals. The oscilloscope records the signal every 0.5μ sec and can store 4096 points in its memory. Its differential plug-in-unit, No.206, designed for recording strain gauge signals is sensitive to 0.05mV. Recorded data can be retrieved from its memory and its stable response can be seen on its screen, even for a transient signal. Besides, any stored signal can be expanded on the oscilloscope screen in either X-axis or Y-axis, upto a magnification of 64. This enables us to focus our attention on the interesting features of a

recorded signal and study them in detail. Voltage at each point can be read directly through a digital display on the oscilloscope screen. Also, hard copies of the recorded signals can be easily obtained on the Hewlett-packard X-Y recorder, No. 7015B.

The output signals from the strain gauges are recorded by a digital oscilloscope. Typical strain gauge records from bar No. 1 and bar No. 2 are shown in Fig. 3.7. The square shaped pulse (input pulse) on the upper trace of Fig. 3.5 is the compressive pulse generated in bar No. 1 by the striker. It has a duration of 116μs and rise time of 16μs. The transmitted tensile pulse is also recorded by the upper trace. This pulse directly indicates the stress at the interface of the specimen and bar No. 1. The lower trace of Fig.3.5, shows the record of compressive input pulse after it passes through the steel collar into bar No.2. This is immediately followed by the incident tensile pulse and the reflected pulse from the interface of the specimen in bar No.2. Note that the reflected and transmitted pulses are time coincident, as the strain gauges are equidistant from the interface of the specimen.

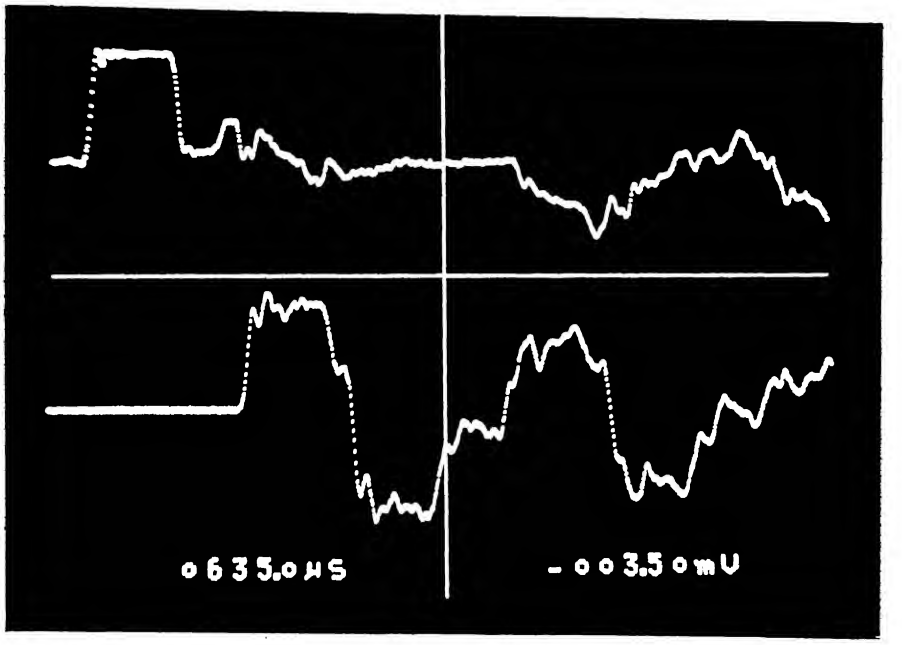

FIG. 3.7 : A TYPICAL OSCILLOSCOPE RECORDS OF THE ALUMINIUM SPECIMEN TESTED BY KOLSKY BAR TECHNIQUE (HARD COPY OF THE OSCILLOSCOPE RECORD IS SHOWN IN FIG. 3.5)

CHAPTER - 4

EXPERIMENTAL RESULTS

Experiments have been carried out mainly on aluminium material to evaluate its stress-strain relations at high strain rates. Specimen for both quasi-static and dynamic testing were machined from a single piece of stock. Aluminium material was chosen from commercially available stock of HINDAL CO., RENUKOT, U.P.. Preliminary experiments have also been carried out on uniaxial glass fiber reinforced plastic composite to determine stress-strain relations in transverse direction. All the experiments have been carried out at room temperature.

Experimental observation involves recording of transient stress pulses on a digital oscilloscope. Specimen were subjected to a loading pulse of duration 116μs with a rise time of 16μs. A rise time of 16μs is large enough to allow the stress to be uniform in the specimen. For every step of 2μs, stress amplitudes of incident, reflected and transmitted pulses were measured and corresponding stress-strain values were evaluated with the help of a digital computer.

4.1 ALUMINIUM SPECIMEN

Six specimens were tested at high strain rates between $410s^{-1}$ and $810s^{-1}$. The results are summarized in Table I along with a quasi-static test at a very low strain rate ($0.2 \times 10^{-3}s^{-1}$).

The quasi-static tensile test was carried out on a standard M.T.S. machine. Load was recorded through a load cell provided in the machine and a differential transformer type extensometer attached across the specimen, monitored the strain. Specimen was made as per ASTM specifications. Resultant stress-strain curve is shown in Fig. 4.1. The specimen yielded at a stress of 172MPa and at a strain of 0.36%. Ultimate stress was 210MPa and ultimate strain was 6.5%. The specimen got fractured and failed due to shear.

Stress-strain curves evaluated using equations (2.22) and (2.23) at various strain rates have been plotted in Fig. 4.1. Specimen 1 was tested at an average strain rate of $410s^{-1}$ and was strained to 4.7%. It can be observed from Fig. 4.1, that the shift of stress strain curve from the quasi-static curve is small, indicating a low strain rate sensitivity at $\dot{\varepsilon} = 410s^{-1}$. The specimen did not fail as the ultimate strain was not attained. The specimen could not be strained beyond 4.7%. One of the methods of attaining ultimate strain

TABLE-I

Specimen No.	Incident pulse duration μs	Stress of Incident tensile pulse MPa	Average strain Rate sec^{-1}	Strain %	Yield stress MPa
1	115	198	410	4.7	188
2	116	214	460	5.2	250
3	114	225	500	5.5	270
4	115	276	560	5.7	330
5	116	301	600	6.5	365
6	115	340	810	8.4	485
7	Quasi-static	-	0.2×10^{-3}	6.5	172

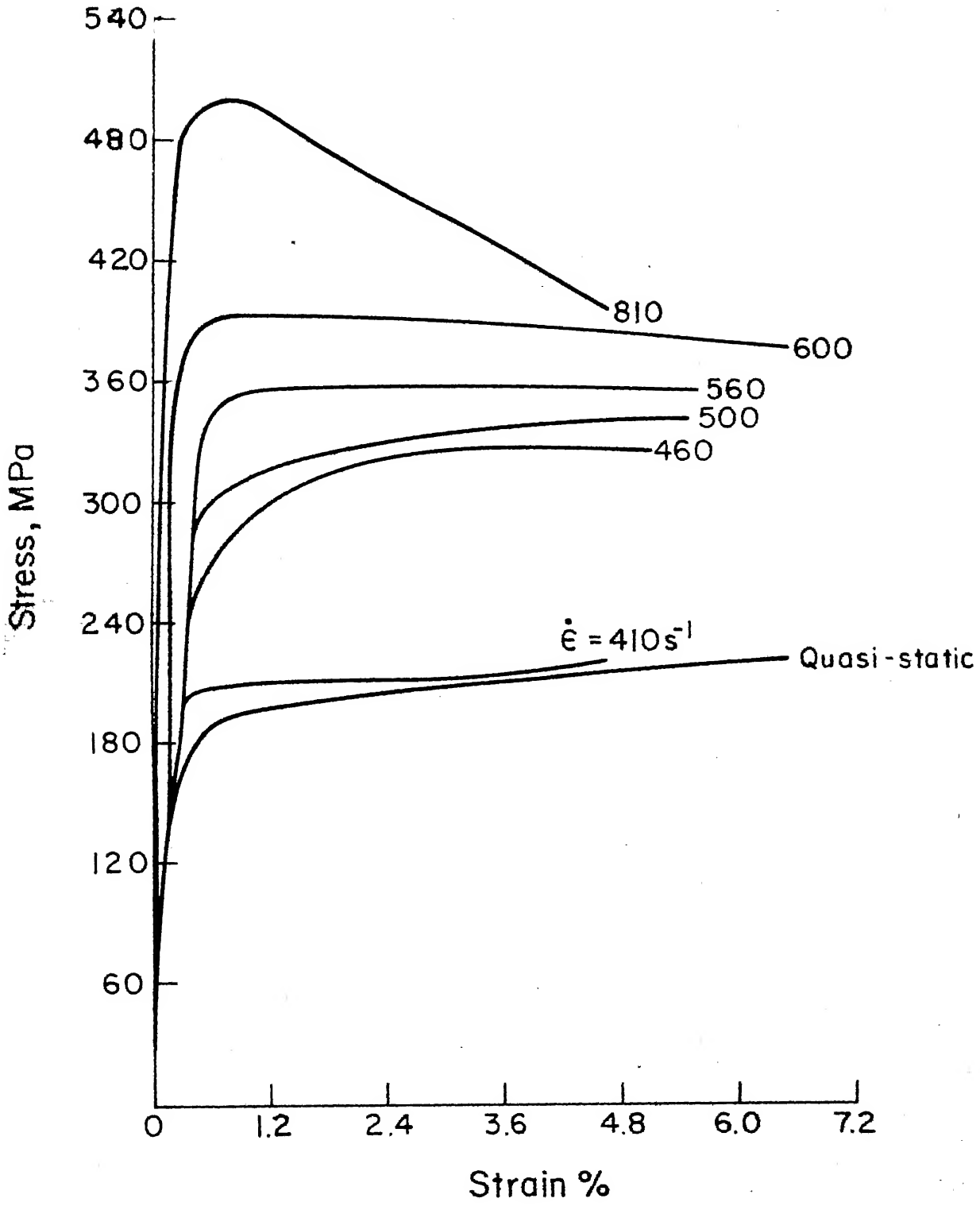

Fig.4.1. Stress-strain curves for aluminium

would be, increasing striker length to increase duration of loading pulse and the length of each bar accordingly, to avoid interference of stress pulses on the recording strain gauges. This was not possible under laboratory conditions due to limitation of space. Alternatively, higher strains could be achieved by decreasing gauge length of the specimen. However, gauge length chosen can not be too small as, deformation in the remaining portions of the specimen start contributing to the deformation within the gauge length. The Kolsky technique cannot account for this deformation separately and hence, the results would not be valid.

Specimen 2 has been impacted at an average strain rate of $460s^{-1}$ and was strained to 5.2%. Considerable upward shift of stress-strain curve from quasi-static curve can be observed from Fig. 4.1. Specimen was subjected to stresses of approx. 47% more than the stresses developed in quasi-static test. At this strain rate the material displayed high strain rate sensitivity. Also, the material showed strain hardening upto 3% strain. The specimen was not loaded until failure.

Specimen 3 was impacted at an average strain rate of $500s^{-1}$ and was strained to 5.5%. The specimen was subjected to stresses which were 55% more than the stresses developed in the quasi-static test. Upward

shift of stress-strain curve,from the stress-strain curve obtained at an average strain rate of $460s^{-1}$ was small. The material strain hardened gradually for the entire duration of the loading pulse. Again, the specimen did not fail during test.

Specimen 4 was impacted at an average strain rate of $560s^{-1}$ and was strained to 5.7%. Upward shift of stress-strain curve can be observed from Fig. 4.1. Specimen was subjected to stresses of 67% more than the stresses developed in the quasi-static test. Process of strain hardening was small upto 1.8% strain and thereafter the material flows without any strain hardening. The specimen did not fail at the applied strain of 5.7%.

Specimen 5 was impacted at an average strain rate of $600s^{-1}$. Decrease in slope of stress-strain curve can be observed, from the point where stress and strain values are 393 MPa and 0.6% respectively, from Fig. 4.1. This phenomenon explains the neck formation in the specimen. As the decrease in the slope is very small, it can be inferred that deformation due to neck formation is not considerable.

Stress-strain values evaluated after the above mentioned point are invalid. Triaxial state of stress

results due to neck formation, which deviates from the basic assumption used in the analysis that, uniaxial state of stress exists in the specimen.

Specimen 6 was impacted at an average strain rate of $810s^{-1}$. Rapid decrease was observed in the slope of stress-strain curve, from the point where stress and strain values are 504 MPa and 0.8% respectively. Specimen 6, with neck formation, is shown along with unstrained specimen in Fig. 4.2. The neck on the loaded specimen was formed at a place close to the centre and well within the gauge length, although it is not very clear from the photograph. Infact, percentage reduction of area is 17%.

It is evident from Fig. 4.1 that the yield stress increases with increasing strain rate. In order to understand the behaviour better, the relation between yield stress and strain is plotted in Fig. 4.3. The behaviour is linear between average strain rates $410s^{-1}$ and $560s^{-1}$. An empirical relation derived to express linear behaviour is

$$\sigma_y = (0.771)\,\dot{\varepsilon} - 121 \qquad (4.1)$$

where σ_y is yield stress in MPa and $\dot{\varepsilon}$ is average strain rate per second. The increase in the slope of straight line in Fig. 4.3, confirms that aluminium is a highly strain rate sensitive material.

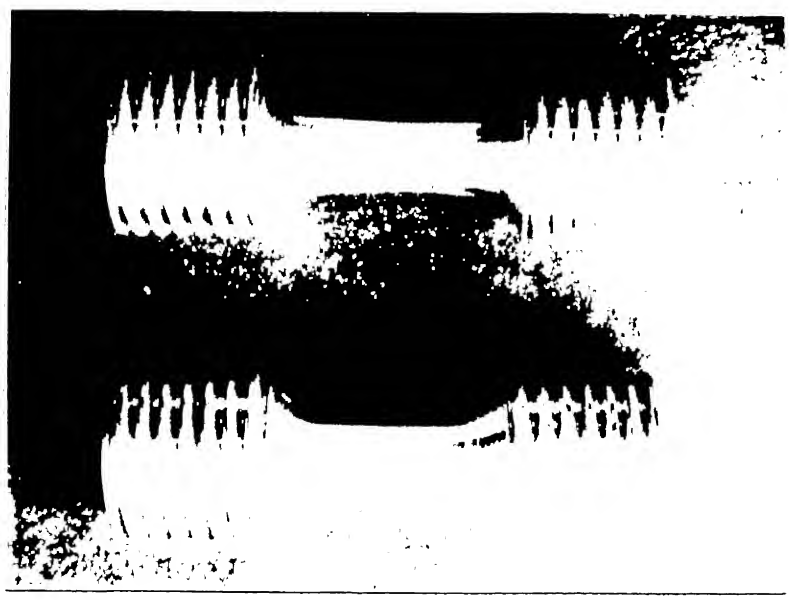

FIG. 4.2 : SPECIMEN NO. 6 (UPPER) DEFORMED AT HIGH STRAIN RATE OF 810s^{-1} AND AN UNTESTED SPECIMEN (LOWER).

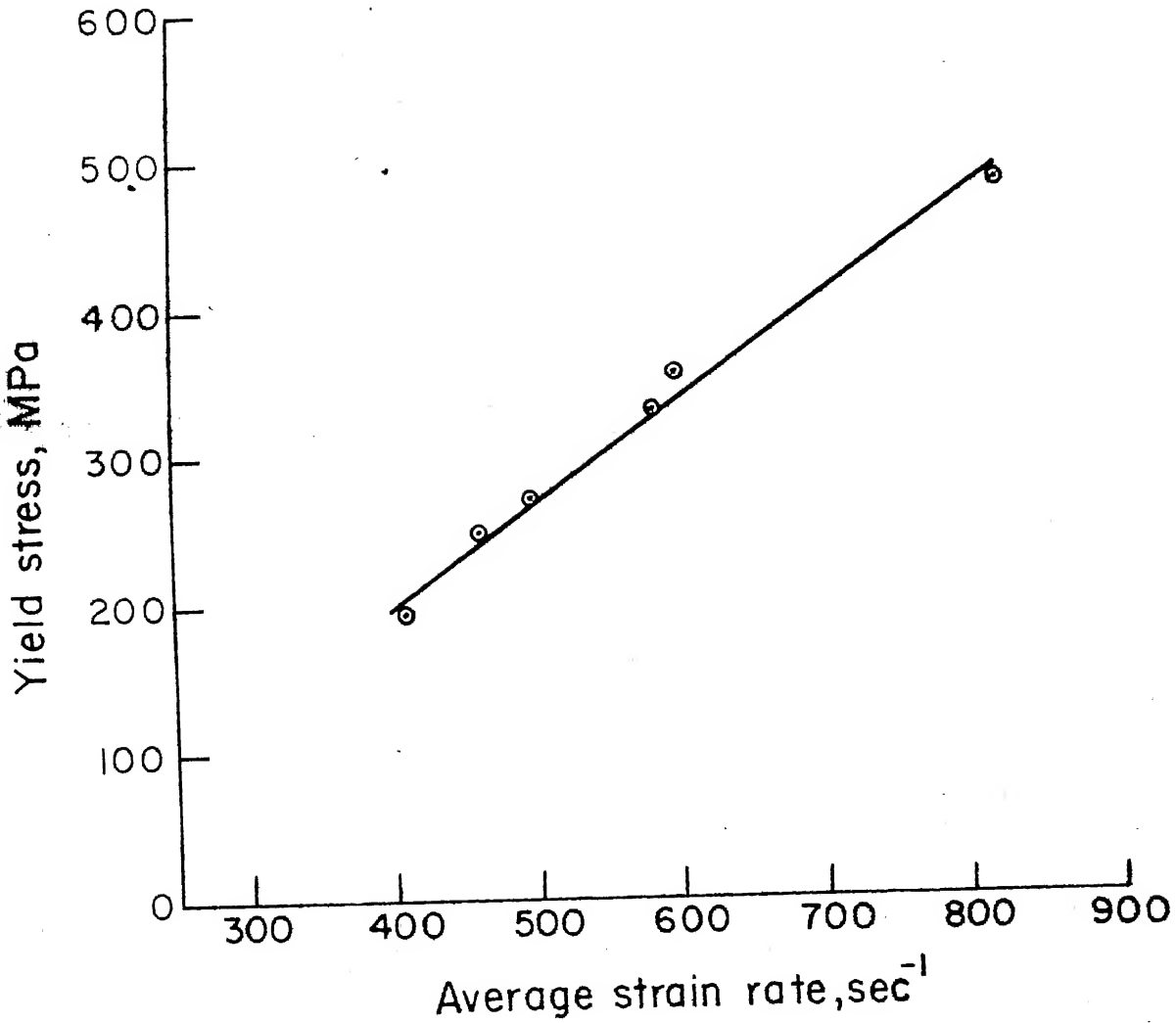

Fig. 4.3 Yield stress vs average strain rate for aluminium

The results of this study are compared with the stress-strain curves obtained by Nicholas[11]. He conducted tests on 6061-T651 aluminium. The dynamic test was carried out at an average strain rate of $600s^{-1}$. The comparision of results is shown in Fig. 4.4 in which, a cross-mark at the end of a curve shows that the specimen failed. Nicholas strained the specimen at an average strain rate of $600s^{-1}$ to failure, by employing a longer duration stress pulse. The material used by Nicholas was different from the material used in this study, in both aspects i.e. impurity content and heat treatment. This is evident from the large difference in the behaviour of quasi static stress-strain curves. Although the materials are different, certain similarities were observed. (i) Both these materials are strain rate sensitive. The material of this study is more strain rate sensitive than 6061-T651 aluminium, as the upward shift of stress-strain curve from quasi-static curve is more, compared to that of Nicholas.(ii) Work hardening at high strain rates specially close to $600s^{-1}$, is negligibly small for both cases, which means that once the dynamic yield stress is crossed, the material at the higher strain rate flows more easily. (iii) Stress-strain curves for both kinds of material, tend to coincide with each other at a high strain rate of

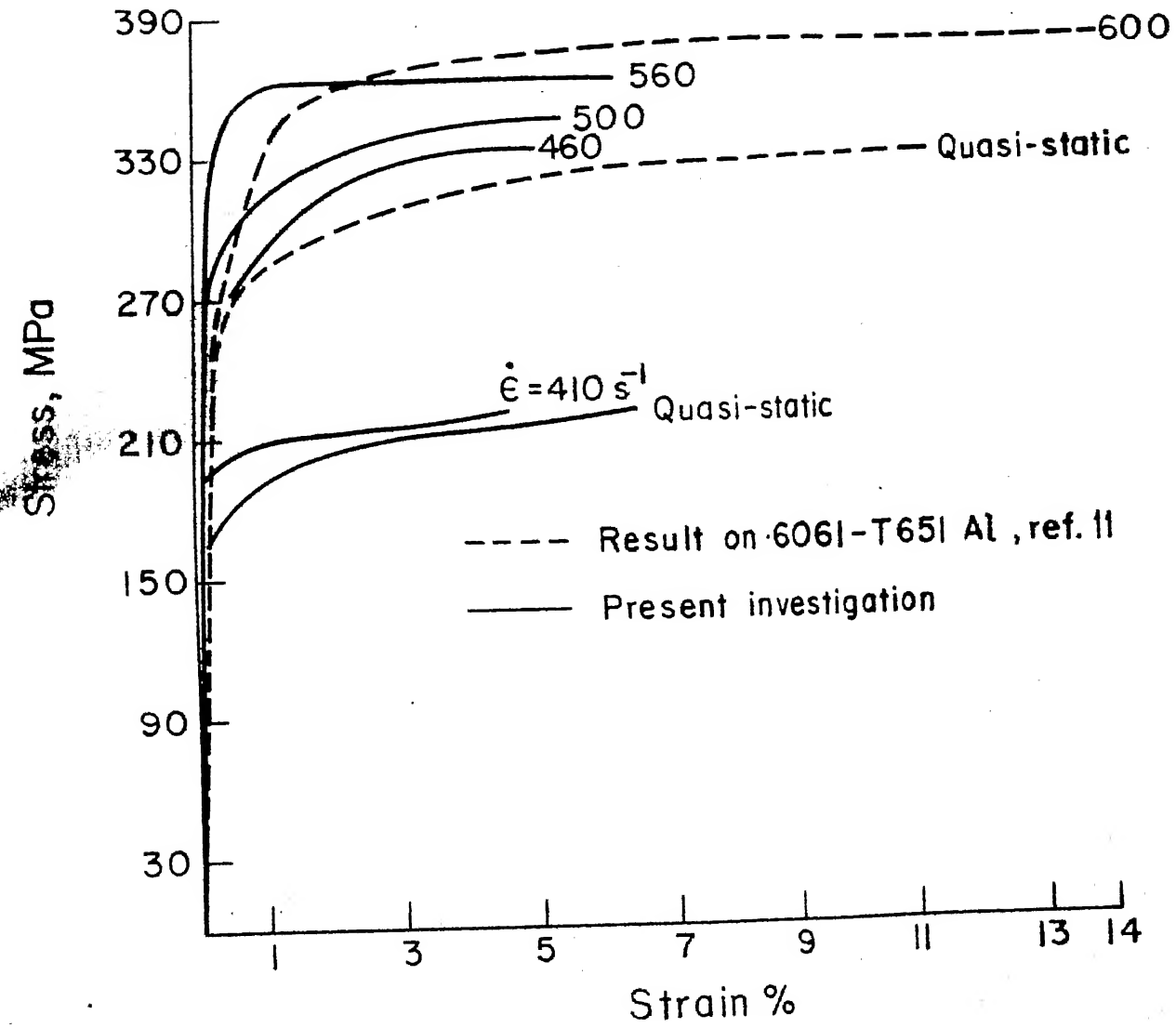

Fig. 4.4. Comparison of results with results of Theodore Nicholas

$560s^{-1}$, which suggests that the stress-strain behaviour does not depend much on the impurity content and heat treatment.

4.2 UNIDIRECTIONAL GLASS FIBRE REINFORCED COMPOSITE SPECIMEN

Fibre reinforced composites now have been realised as feasible materials for structural purposes due to their attractive properties such as high strength to weight ratio, ease of forming process, corrosion resistance etc. These composites are used to manufacture high speed aircraft, missiles, space ships, marine industry or other structures subjected to blast or shock wave loadings. Jet engine and helicopter blades made of composite materials are exposed to the hazards of bird impact and thus causing extensive damage to the blade. In view of this, the designers and researchers require a thorough knowledge of stress-strain behaviour of composites at high rate of loading.

Dynamic tension test was carried out on 90° glass fiber reinforced composite. The specimen was machined from a composite plate, with an approx. volume fraction of 37%. A 21 mm composite plate was cast using Cy 230 Resin and Hy 951 Hardner. Dimensions of the specimen are given in Fig. 3.2.

The specimen was subjected to an average strain rate of $110s^{-1}$ and was strained to 0.66%. Ultimate strain was not attained, as the specimen failed near the grips. The specimen was subjected to an incident tensile pulse of magnitude 77MPa. As stress levels were very low, the recording of transmitted pulse was not accurate due to surrounding electrical noise problems. The preliminary results of a dynamic stress-strain curve at an average strain rate of $110s^{-1}$ are presented in Fig. 4.5. At low strain (upto 0.4%) the modulus is 3.2 GPa. However, for strains, above 0.4%, the stress-strain curve of Fig. 4.5 is concave. Though this kind of behaviour is usually observed in materials like rubber, is unusual for epoxy-resin or glass fiber. The behaviour of stress-strain curve, might have been the result of inaccurate recording of feeble stress pulse by strain gauges. Further investigation would have to be carried out, to confirm the dynamic behaviour of 90° glass fiber composite.

4.3 SUMMARY

The dynamic tension tests confirm, that at room temperature, commercial aluminium of HINDALCO is a strain rate sensitive material. Stress-strain curves shift upwards with increasing strain rate. Strain hardening

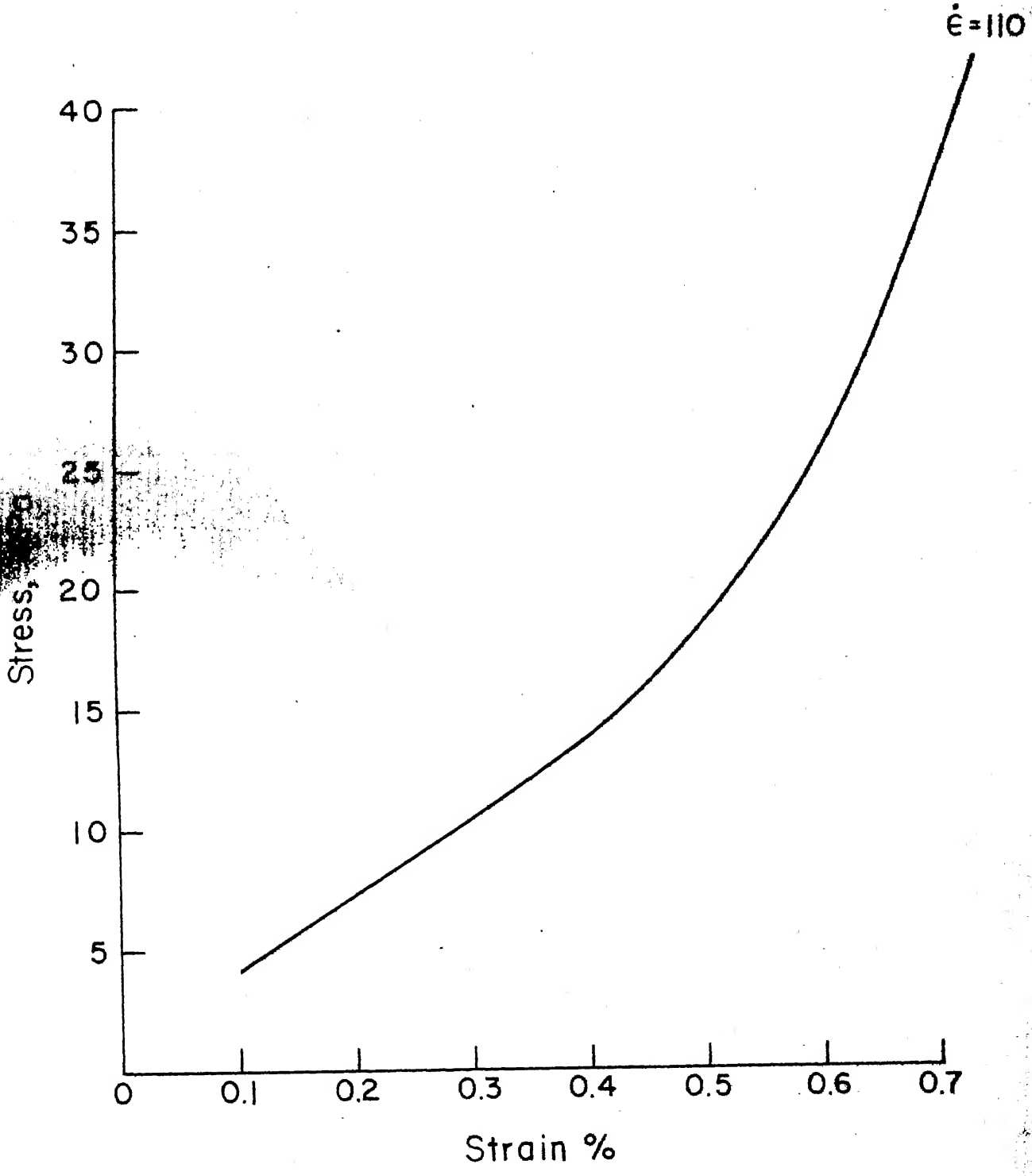

Fig. 4.5 Transverse tension test on a uniaxial GFRP specimen

is small, specially at a high strain rate of the order $560s^{-1}$. A linear relation between yield stress and average strain rate has been observed and the yield stress increases appreciably with increasing strain rate.

Stress-strain curve of a preliminary nature, has been obtained on glass fiber composite specimen, in the transverse direction.

CHAPTER - 5

CONCLUDING REMARKS

The primary objective of setting up an apparatus to conduct high strain rate tensile testing and to evaluate material behaviour was successfully met with. To carry out Kolsky pressure bar technique, pressure bars were designed and fabricated. Strain gauges were attached to record dynamic stress pulses for subsequent analysis. Specimen were subjected to a loading pulse of approximately 116μs duration.

Tests have been conducted on commercially available aluminium metal and stress-strain relations have been evaluated at various strain rates. Aluminium was found to be strain rate sensitive. A linear relation was observed between the yield stress and average strain rate. The yield stress increased appreciably with an increase in average strain rate. Furthermore, the aluminium metal flows with negligible strain hardening at a high strain rate of $560s^{-1}$.

Most of the aluminium metal specimen of this study could not be strained to failure because, a pulse

of 115μs duration available in the present setup was not long enough. Therefore, it is recommended that, the duration of loading pulse be increased by increasing the length of striker bar and correspondingly increasing the lengths of the pressure bars.

To understand the dynamic behaviour of unidirectional glass fibre composite, dynamic tests have to be conducted mainly in two principal directions i.e. longitudinal and transverse. The limitations in the present setup to study dynamic behaviour in the transverse direction are:

(i) Strength of the specimen decreased at the grips, as a result of cutting threads which were acting like cracks. Hence, the specimen failed at the grips while being loaded in tension.

(ii) Tensile strength in the transverse direction was low, producing feeble stress pulses, which resulted in, inaccurate recording by strain gauges.

Also, the present setup could not be used to study the dynamic behaviour in the longitudinal direction because, threads on the specimen could not be cut due to tearing of fibers.

The suggested modifications, to study dynamic behaviour of glass fiber composite material are:

(i) The gripping arrangement to hold the specimen has to be modified. One of the solutions can be to use a specimen with a rectangular cross-section. Then, a serrated type of jaws, similar to that of a UTM, can be developed to hold the specimen between the pressure bars.

(ii) To increase the sensitivity of strain gauge circuits, strain gauges of higher resistance can be used.

(iii) By using the pressure bars made of lower modulus material, such as aluminium alloy, which remains elastic during the test but provides a larger strain for the same loading pulse.

REFERENCES

1. Kolsky, H., " An Investigation of Mechanical Properties of Materials at Very High Rates of Loading", Proceedings of Physical Society, Series B, Vol. 62 (1949) PP 676-700.

2. Davies, E.D.H., and Haunter, S.C., " The Dynamic Compression Testing of Solids by the Method of Split Hopkinson Pressure Bar", J. Mech. and Phys. of Solids, Vol. 11 (1963) PP 155-179.

3. Barker, L.M., and Hollenbach, R.E., " System for Measuring the Dynamic Properties of Materials", J. App. Mechanics, Vol. 35, No. 6 (1964), PP 742-766.

4. Campbell, J.D., and Maiden, C.J., " The Effect of Impact Loading on the Static Yield Strength of Medium Carbon Steel", J. Mech. and Phys. of Solids, Vol. 6 (1957) PP 53-62.

5. Lindholm, U.S., " Some Experiments With Split-Hopkinson Bar", J. Mech. and Phys. of Solids, Vol. 12 (1964) PP 317-335.

6. Hauser, Frank, E., " Techniques for Measuring Stress-Strain Relations at High Strain Rates", J. Experimental Mechanics, Vol. 6, No. 8 (1966) PP 395-402.

7. Lindholm, U.S., and Yeakley, L.M., " High Strain Rate Testing: Tension and Compression", J. Experimental Mechanics, Vol. 3 (1968) PP 1-9.

8. Dharan, C.K.H., and Hauser, F.E., "Determination of Stress-Strain Characteristics at Very High Strain Rates", J. Exptl. Mechanics, Sept. (1970) PP 370-376.

9. Jahsman, W.E., " Re-examination of Kolsky Technique for Measuring Dynamic Material Behaviour", J. App. Mech., Vol. 38, Series E, (1971) PP 75-82.

10. Gorham, D.A., " Measurement of Stress-Strain Properties of Strong Metals at Very High Rates of Strain", Institute of Physics Conf. Ser No.47: Chapter 1 (1979) PP 16-24.

11. Nicholas, T., " Tensile Testing of Materials at High Rates of Strain", J. Exptl. Mechanics May (1981) PP 177-185.

12. Alder, J.F., and Phillips, V.A., " The Effect of Strain Rate and Temperature on Resistance of Aluminium, Copper and Steel to Compression", J. Institute of Metals, Vol 83 (1954-55) PP 80-84.

13. Lundergan, C.D., " Equation of State of 6061-T6 Aluminium at Low Pressures", J. App. Phys., Vol. 34, Number 7 (1963) PP 2046-2048.

14. Malvern, L.E., " Experimental Studies of Strain Rate Effects and Plastic Wave Propagation in Annealed Aluminium", Trans. ASME, NEW YORK (1965) PP 81-92.

15. Amijima, S., and Fujii, T., " The Impact Compressive Testing of Chooped Strand Glass Mat. Laminated Composites by the Split-Hopkinson Pressure Bar Method", Proc. of Nineteenth Japan Congress on Material Research, Published by "The Society of Materials Science", Kyoto, Japan, 1976.

16. Chimmalgi, V.S., " Experimental Study of Stress-Strain Behaviour of Epoxy at High Strain Rate", M. Tech. Thesis, Department of Mechanical Engg., I.I.T. Kanpur, 1981.

17. Nakarani, R.K., " High Velocity Impact Properties of Unidirectional GFRP" , M. Tech. Thesis, Department of Mechanical Engg., I.I.T. Kanpur, 1983.